Donaldson
Filtration Solutions

Effect of Surface Area, Pore Size, and Surface Chemistry of Activated Carbon on Removing Low Concentrations of Volatile Organic Contaminants

Austrailia • Austria • Belgium • Canada • China • Czech Re
Denmark • France • Germany • Hungary • India • Indones
Japan • Malaysia • Mexico • Netherlands • New Zealand
Poland • Saudi Arabia • Singapore • Slovakia • South Afri
South Korea • Spain • Sweden • Switzerland • Taiwan • Th
Turkey • United Arab Emirates • United Kingdom • United S

Disk Drive

Effect of Surface Area, Pore Size, and Surface Chemistry of Activated Carbon on Removing Low Concentrations of Volatile Organic Contaminants

Andrew J. Dallas,[*a] Lefei Ding,[a] Jon Joriman,[a] Dustin Zastera,[a] and Gerald Weineck[b]
[a]Donaldson Co., Inc., Corporate Technology, 9301 James Ave., Bloomington, MN 55431
[b]Donaldson Co., Inc., Disk Drive, 9301 James Ave., Bloomington, MN 55431

ABSTRACT

Three activated carbon samples that are commonly applied in chemical filters are shown to differ significantly in their surface area, pore size distribution, and surface chemistry. The surface properties of these carbons were characterized by: 1) nitrogen, toluene, and water adsorption isotherms; 2) Energy Dispersive Spectroscopy (EDS); 3) pH titration; 4) temperature programmed inverse gas chromatography; and 5) packed bed breakthrough curves. The infinite dilution gas chromatography results were evaluated using Linear Free Energy Relationships (LFERs) in order to rationalize the surface chemical properties that govern adsorption/desorption of volatile organic contaminants (VOCs) from the carbon surface. These model results are then used to predict the relative performance of the three activated carbons for removing low concentrations of seven Test VOCs.

1. INTRODUCTION

Chemical filters containing activated carbon are very effective at controlling volatile organic contaminant (VOCs) levels in a wide range of industrial and commercial applications. The VOC type and concentration can vary widely by application. The physical and chemical properties of the adsorbent that govern surface adsorption and desorption are also known to vary with the contaminant (adsorbate) type and concentration; thereby significantly complicating the process of selecting an adsorbent.[1-16] Usually, this choice is based on a comparison of adsorbent surface characteristics such as surface area, pore volume, and pore size. Rarely, are the contaminant and adsorbent surface chemical properties taken into account.

Only recently has the importance of pore structure, pore size distribution, and surface chemistry of activated carbons been discussed and their significance to chemical filter performance been investigated.[12, 15, 17-19] At high adsorbate concentrations, surface area and pore volume dominate activated carbon capacity; however, the interrelated nature of the pore size distribution and surface chemistry become critical for optimum performance at lower concentrations. By low concentration we refer to a concentration that is essentially infinitely dilute, or where adsorption takes place to the point of forming less than a monolayer of adsorbate on the adsorbent surface and micropores become filled. Understanding this cooperative process in activated carbon has proven crucial in designing chemical filter systems for hard disk drives, fuel cells, semiconductor tools, full FAB filters, sensors, pressure and thermal swing driers, dilution air purification systems, and cabin air. In these applications adsorbate concentrations can range from sub parts per billion (ppbv) to low parts per million (ppmv).

The distribution of pore sizes within an adsorbent can significantly affect adsorption of VOCs. Enhanced adsorbate-adsorbent interactions occur in pores of molecular dimension. A decrease in pore width results in an increase in the adsorption energy and a decrease in the concentration at which a specific pore size becomes filled.[1] These "higher-energy" pores (e.g. micropores) are therefore filled at low concentrations. In these smaller pores, an increase in the adsorption energy results due to increased contacts between the adsorbate and the adsorbent surface, as well as the adsorbate experiencing an overlap of the adsorption potentials of opposing pore walls. Since, granular and beaded activated carbons typically exhibit a heterogeneous pore structure, capacity at low adsorbate concentrations will be related to the extent that the pore network is microporous.

[*] andrewd@corptech.donaldson.com; phone 1 952 887-3318; fax 1 952 887-3937; http//www.donaldson.com

Equally as important as the pore size distribution, there exists on the activated carbon adsorbent and specifically at the edges of the micropores, atoms and functional groups other than carbon. These sites are considered to be higher energy adsorption sites and are typically comprised of oxygen, nitrogen, sulfur and the halogens. Oxygen is probably the most important, since it is commonly found on activated carbon surfaces as a result of the activation process.[3] Adsorbates are initially adsorbed on an adsorbent's highest energy sites, and once saturated, adsorption commences by pore filling and capillary condensation.[1] Hence, the adsorbent surface chemistry will dictate its ability to adsorb specific contaminants at ppbv and ppmv levels.

The activated carbon backbone structure is typically a polyaromatic carbon sheet that contains specific functional groups along its edges.[3] This surface chemistry gives rise to a polar surface. An acidic surface results from the presence of oxygen in the form of carboxylic acid, phenolic, and hydroxyl groups. Oxygen is also found on activated carbon surfaces in the form of carbonyl and ether functional groups, which tends to add a basic character to the surface. Heat treatment in inert atmospheres effectively removes these groups, resulting in a less polar surface.

The aim of this work is to characterize the pore structure and surface chemistry of three activated carbons using: 1) the sorption of nitrogen, toluene, and water; 2) Energy Dispersive Spectroscopy (EDS); 3) pH titration; and 4) temperature programmed inverse gas chromatography. Additionally, it focuses on rationalizing the adsorbate-adsorbent interactions that govern adsorption and desorption on these activated carbon materials using Linear Free Energy Relationships (LFERs). This information is then used to estimate their relative performance for removing seven Test VOCs from an airstream.

1.1. Theoretical Background of Temperature Programmed Inverse Gas Chromatography and Linear Free Energy Relationships:

Gas-solid chromatography, when applied to the investigation of solid surface properties is usually called inverse gas chromatography (IGC). At infinitely dilute adsorbate concentrations, it is assumed adsorption can be described by Henry's Law; therefore, retention in gas-solid chromatography is directly related to the total free energy of adsorption, ΔG_{ads}.[11,20] ΔG_{ads} is a measure of the adsorbate-adsorbent interactions and its magnitude is dependent on the nature of both the adsorbate and the adsorbent. These interactions are generally assumed to involve two types of interactions, dispersive (nonspecific) and polar (specific), that are independent and additive:

$$\Delta G_{ads} = \Delta G_{ads}^{d} + \Delta G_{ads}^{p} \qquad \textbf{(1)}$$

where, ΔG_{ads}^{d} is the dispersive interaction contribution to the free energy of adsorption and ΔG_{ads}^{p} is the polar interaction contribution to the free energy of adsorption. Polar interactions include orientation, induction, and hydrogen bonding. Both dispersive and polar interactions make favorable contributions to ΔG_{ads} and can be separated as is shown in Figure 1.[21] ΔG_{ads}^{p} can be calculated by subtracting ΔG_{ads}^{d}, determined from the "reference alkane line", from ΔG_{ads}. These basic IGC principles are typically used to investigate adsorbate-adsorbent interactions and in combination with LFERs that have been shown to readily provide estimates of the magnitude of these interaction energies.

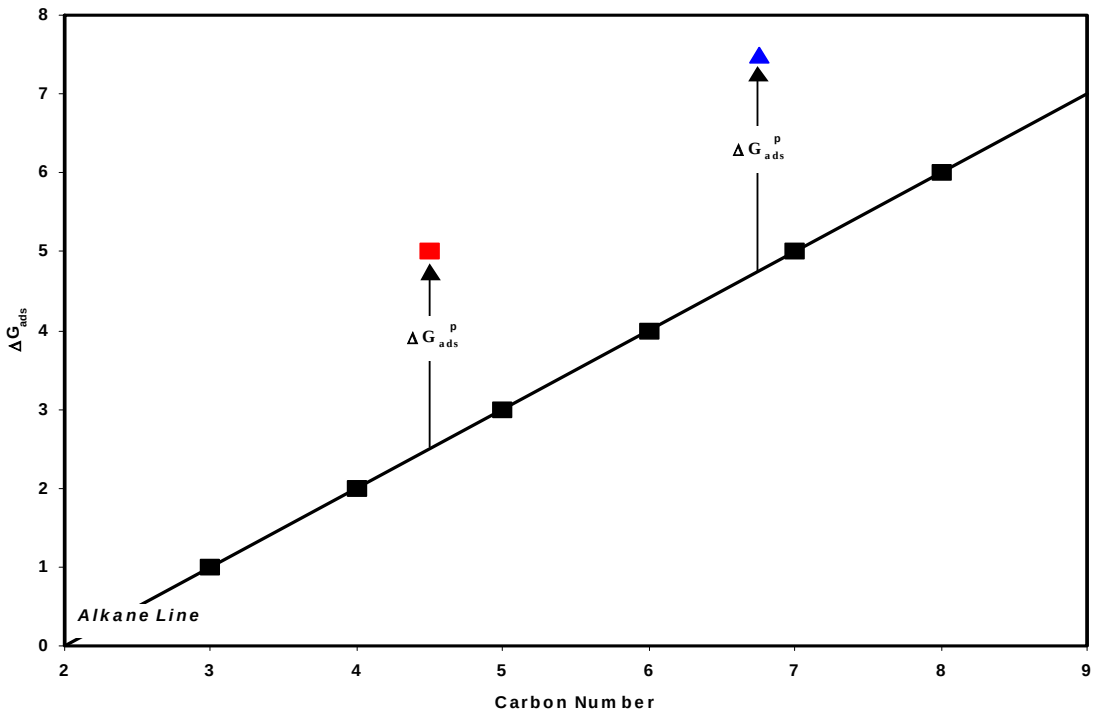

Figure 1: Principles of the contributions made by the dispersive (nonspecific) and polar (specific) free energies of adsorption to the total free energy of adsorption.

Generally, isothermal IGC has been used to characterize adsorbent surfaces and several authors have used it in combination with LFERs to study activated carbon surfaces. [5, 8, 11, 22, 23] However, the heterogeneous nature of the activated carbon surface and the extensive microporous structure limits the range of adsorbates and temperatures that can be evaluated. As a result of these strong specific interactions, poor adsorbate peaks shapes are generally obtained. These poor peak shapes along with the limited sensitivity of chromatographic detectors make it difficult to carry out adsorption studies at infinitely dilute concentrations when using isothermal conditions.

In a similar vein as McMahon et al,[24] we have attempted to extend the "classical" IGC approach for studying adsorbent surfaces using temperature-programmed gas chromatography. These methods allow us to evaluate adsorption at adsorbate concentrations at lower concentrations than is possible by isothermal techniques. Additionally, they simplify and speed-up the data collection process. In our approach, a series of twelve judiciously chosen probe adsorbates are individually injected into a column packed with activated carbon. Upon injection the column is initially set to a low temperature and is subsequently ramped using a slow temperature ramp of 4°C/min. The temperature is increased until the adsorbate has completely eluted from the column. The peak elution temperature, T_R, for each adsorbate is directly related its ΔG_{ads} on the activated carbon column packing. Although, the absolute value of an adsorbate's ΔG_{ads} cannot be determined from a single run; however, relative values can be obtained by comparing the elution temperature for a series of probe adsorbates. From these elution temperatures a greater understanding of the nonspecific and specific interactions can be obtained.

LFERs have been used extensively in the literature to discern the phase transfer properties of many liquid-liquid, gas-liquid, and gas-solid systems. They will be used here in an attempt to rationalize the chemical and physical factors that govern the adsorption and desorption of VOCs on activated carbon. LFERs are applied to the elution temperature results of twelve judiciously chosen adsorbates on three activated carbon materials.

In the LFER approach, a free energy related measurement, such as the elution temperature, is used as the dependent variable and is regressed against a series of probe molecule descriptors defined by Abraham et al.

$$T_R = SP_o + \boldsymbol{l} \log L^{16} + \boldsymbol{r} R_2 + \boldsymbol{s} \pi_2^H + \boldsymbol{a} \Sigma\alpha_2^H + \boldsymbol{b} \Sigma\beta_2^H \quad (2)$$

or

$$T_R = SP_o + \boldsymbol{m} V_x + \boldsymbol{r} R_2 + \boldsymbol{s} \pi_2^H + \boldsymbol{a} \Sigma\alpha_2^H + \boldsymbol{b} \Sigma\beta_2^H \quad (3)$$

where, T_R represents the free energy related measurement and the probe adsorbate descriptors are: 1) L^{16}, the gas-hexadecane partition coefficient used to model the adsorbate size and dispersive interactions; 2) R_2, adsorbate excess molar refraction, which reflects an adsorbate's ability to interact with an adsorbent through π- and n-electron pairs; 3) π_2^H, adsorbate dipolarity/polarizability; 4) $\Sigma\alpha_2^H$, solute hydrogen bond donor acidity; and 5) $\Sigma\beta_2^H$, solute hydrogen bond acceptor basicity.[11, 26, 27] In the case of equation 3, V_x is the McGowan characteristic volume that is calculated from the molecular structure.[28]

SP_o, ***l*** or ***m***, ***s***, ***d***, ***a*** and ***b*** represent the intercept and the regression coefficients from Equations 2 and 3. The magnitude of the regression coefficients is representative of the properties of the adsorbent surface. For example, the ***s*** coefficient indicates the degree to which the adsorbent surface can interact with the infinitely dilute adsorbates through dipole-dipole and dipole-induced dipole interactions. A relatively large positive value of a coefficient indicates that this interaction contributes to the adsorption process. By comparing the LFER coefficients for a series of adsorbents it is possible to rationalize the relative importance of nonspecific and specific adsorbate-adsorbent interactions on each adsorbent.

Equation 2 has been recommended for processes involving the gas-liquid, or gas-solid, transfer of probe molecules.[5, 11, 22, 23] The use of L^{16} in this equation is understood to take into account the difference in the cavity formation process between the gas and liquid phases; as well as accounting for the difference in dispersive interactions in either phase. Equation 3 is typically recommended for processes involving the liquid-liquid transfer of probe molecules, where it is thought that the dispersive interaction essentially cancel in the two liquid phases and there is only a need for a size, or cavity, related term.

Based on these interpretations, Equation 2 has typically applied in the LFER evaluation of retention measurements on graphite, carbon molecular sieves, and activated carbons.[5, 8, 11, 22, 23] In most cases, relatively poor regressions are obtained and specific polar interactions are insignificant.[11, 22, 23] It has been suggested that the following LFER equation involving only nonspecific adsorbate-adsorbent interactions can be applied when evaluating gas-solid adsorption on heterogeneous surfaces:

$$T_R = SP_o + \boldsymbol{l} \log L^{16} + \boldsymbol{r} R_2 \quad (4)$$

In addition to the apparent lack of specific interactions in gas-solid interactions in this equation, when used, an unfavorable contribution to the free energy of adsorption is obtained for the interaction of an adsorbate with an adsorbent through π- and n-electron pairs. This unfavorable contribution is indicated by a negative value of the ***r*** coefficient.[5, 11, 22, 23] It has previously been pointed out that the lack of specific interactions is obviously incorrect.[8] This work will attempt to resolve these discrepancies and show that specific interactions play a significant role in adsorption of VOCs on activated carbon at ppbv and ppmv concentrations. It will be shown that a negative ***r*** coefficient does not make sense in the case of gas-solid adsorption on activated carbon.

2. EXPERIMENTAL

Three activated carbons were used without further modification except for the sample preparation required by the respective measurement being employed as described below. These carbons are identified in this work using the

same designations given in reference 12. Carbon B is a wood-based activated carbon. Carbons C and F are coconut shell-based activated carbons.

2.1. Nitrogen Adsorption:

Nitrogen adsorption isotherms were used to determine the BET surface area, pore volume, and micropore area of the three activated carbon materials. These nitrogen adsorption isotherms were further analyzed using Density Functional Theory (DFT) to determine the relative pore size distribution for each activated carbon sample.[29, 30]

The activated carbon samples were prepared for nitrogen adsorption by out-gassing them overnight at elevated temperature under high vacuum. Nitrogen adsorption isotherms were measured at –196°C, using standard continuous flow conditions on a Micromeritics ASAP 2010 instrument.

2.2. Toluene Adsorption:

Toluene, an important environmental contaminant, was chosen as one of our probes of the pore structure and specific polar/nonpolar interactions between contaminants and activated carbon surfaces.[12] Adsorption isotherms were measured over the toluene concentration range of 5-35,000 ppm using gravimetric methods similar to the methods of Graf et al.[25] A schematic of the general experimental setup is given in Figure 2.

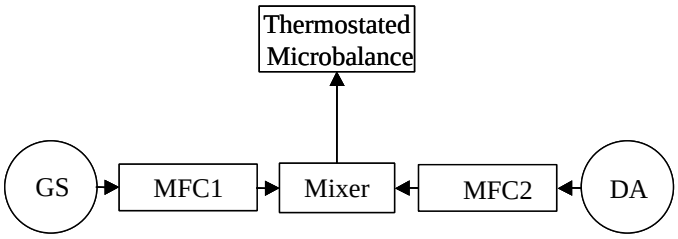

Figure 2: Schematic of adsorption isotherm experiment. GS = toluene; MFC1/2 = mass flow controllers; DA = dilution air.

Two separate gravimetric approaches were used to determine the adsorption isotherm over the entire concentration range: 1) a TA Instruments 951 thermalgravimetric analyzer (TGA) for toluene concentrations lower than 100 ppmv; and 2) a VTI SGA-100 symmetric vapor sorption analyzer for toluene concentrations greater than 100 ppmv.

The activated carbon samples were prepared by outgassing them at elevated temperature under high vacuum. Adsorption isotherms were determined at 25°C (±0.5°C) using constant temperature water baths to control the temperature of the sample chambers. For the TGA measurements, a cooling device was designed to work in conjunction with a water bath to control the temperature of the TGA sample chamber.

2.3. Water Adsorption:

Water adsorption-desorption isotherms from 15-95% relative humidity (%RH) were determined gravimetrically at 25°C. Measurements were made using a VTI-SGA-100 symmetric vapor sorption analyzer. The activated carbon samples were prepared by outgassing them at elevated temperature under high vacuum.

2.4. pH of the Carbon Surface:

The pH of the activated carbon surface was measured using ASTM D-3838-80 as the basis for the method. Ten grams of activated carbon and 100mL of DI water are added to a 250mL round bottom boiling flask. This flask is attached to a Liebig condenser and gently boiled for 20 minutes. The liquid is filtered through a nylon 0.2 µm disposable filter and cooled in a polypropylene bottle. The filtrate's pH is determined using a calibrated Orion

model 720A pH meter. The average of three samples was taken to represent the pH of the activated carbon adsorbent.

2.5. Energy Dispersive Spectroscopy of Carbon Surface:

A JEOL JSM-5900LV scanning electron microscope with a JEOL 5900 EDAX attachment was used to make the activated carbon surface elemental measurements. After drying at 60°C under vacuum, the activated carbon samples were mounted onto metal stubs using carbon tabs for EDS elemental analysis. The samples are then analyzed using EDS under low vacuum and a backscatter detector. Scans were taken at five different locations on each activated carbon sample. The average of these five scans is taken as being representative of the elemental composition of the activated carbon surface.

2.6. Inverse Gas Chromatography/Linear free energy relationships:

The infinite dilution elution temperature, T_R, of twelve judiciously chosen probe adsorbates were measured using temperature programmed gas chromatography. These adsorbates were chosen so as to span a wide range in chemical properties. These twelve adsorbates along with the seven Test VOCs are given in Table 1 along with their LFER descriptors.

Table 1: Adsorbate and Test VOC LFER Descriptors:

Adsorbates	V_x	R_2	π_2^H	$\Sigma\beta_2^H$	$\Sigma\alpha_2^H$	Log L^{16}
n-Butane	0.6722	0.000	0.00	0.00	0.00	1.615
n-Pentane	0.8131	0.000	0.00	0.00	0.00	2.152
n-Hexane	0.9540	0.000	0.00	0.00	0.00	2.670
n-Propanol	0.5900	0.236	0.42	0.48	0.37	1.984
1,1,1,3,3,3-Hexafluoroisopropanol	0.6962	-0.240	0.55	0.10	0.77	1.253
Diethyl Ether	0.7309	0.041	0.25	0.45	0.00	2.040
Acetonitrile	0.4042	0.237	0.90	0.33	0.04	1.479
Propionitrile	0.5451	0.162	0.90	0.36	0.02	1.960
Butyronitrile	0.6860	0.188	0.90	0.36	0.00	2.456
Methylene Chloride	0.4943	0.387	0.57	0.05	0.10	2.013
Benzene	0.7164	0.610	0.52	0.14	0.00	2.799
Nitromethane	0.4237	0.313	0.95	0.31	0.06	1.808
Test VOCs						
Sulfur Dioxide	0.3465	0.370	0.66	0.10	0.28	0.778
Ammonia	0.2084	0.139	0.35	0.62	0.14	0.208
n-Propane	0.5313	0.000	0.00	0.00	0.00	0.531
Toluene	0.8573	0.601	0.52	0.14	0.00	0.857
Ethanol	0.4491	0.246	0.42	0.48	0.37	0.449
Acetaldehyde	0.4061	0.208	0.67	0.45	0.00	0.406
Water	0.1673	0.000	0.45	0.35	0.82	0.167

A Shimadzu Mini-GC2 gas chromatograph with a direct injection port and liner were used to measure T_R. The activated carbon samples were sieved to a mesh size of 60-80 mesh in order to minimize particle size effects. The sieved carbon samples were packed into Silcosteel coated ¼ inch stainless steel tubes of similar length. The packed columns were connected between the injection port and the flame ionization detector. Purified nitrogen was used as the carrier gas at a flow rate of 30 cm^3/min. The column was conditioned by ramping the temperature up to 300°C and holding it for one hour. The column was then cooled to 35°C. Head-space samples of the adsorbates were injected into the heated injection port using a 10 μl gas tight syringe. Upon injection of the adsorbate, the temperature was immediately increased at a ramp rate of 4°C/min until the entire adsorbate peak eluted. The amount of adsorbate head-space that was injected was decreased until a constant elution temperature was obtained.

The average of three separate measurements of the elution temperature of each adsorbate was taken as its value of T_R.

The average T_R values for each all twelve adsorbates were regressed against the adsorbate descriptors given in Table 1 using equations 2 and 3.

2.7. Breakthrough Curves:

The removal efficiency and capacity of a given chemical filter is typically determined by measuring a series of breakthrough curves. A 12 x 20 mesh sample of each of the activated carbons was placed in a temperature controlled sample holder. The temperature of the sample was controlled to 25°C (±0.2°C) using a constant temperature water bath. Samples were conditioned in the sample chamber by purging them with a purified air stream controlled at 50%RH for a minimum of one hour. The Test VOCs were delivered to the sample chamber at 30 LPM after diluting either a concentrated certified standard gas or a saturated airstream with purified air to achieve a concentration of 50 ppmv; except for acetaldehyde, which involved the dilution of permeation tube emissions to a concentration of 6.0 ppmv. All flows were controlled using mass flow controllers (Aalborg). Breakthrough of the VOCs was detected by either a flame ionization detector (JUM Engineering, Total Hydrocarbon Analyzer, Model VE7) or an FTIR (ThermoEnvironmental Instruments, MIRAN SapphIRe).

3. RESULTS AND DISCUSSION

3.1. Nitrogen Adsorption:

The BET total surface area, pore volume, average pore diameter, and micropore area for the three activated carbons are given in Table 2.

Table 2: Physical properties of activated carbon materials as determined by nitrogen BET analysis.

Activated Carbon	BET Total Surface Area (m^2/gr)	Pore Volume (cm^3)	Micropore Area (m^2/gr)	Average Pore Diameter (Å)	Ratio[a] (MA/SA)
Carbon B	1689	1.17	142	28.6	0.08
Carbon C	1530	0.74	984	16.9	0.64
Carbon F	928	0.48	771	19.4	0.83

a. Ratio of micropore area to the total surface area.

The wood-based activated carbon, Carbon B, has the highest BET total surface area and the lowest micropore area. Carbon F has the highest percentage of micropores as indicated by the ratio of the micropore area to the total surface area.

The DFT pore size distributions of the three activated carbon materials, for pore diameters of less than 25Å, are given in Figure 3. Although Carbon B possesses some of the smallest pores, most of its pore volume results from pores with diameters greater than 10Å. Conversely, the pore volume for Carbon F primarily comprises pores with diameters of less than 10Å, and mostly less than 6-7Å. Carbon C has a relatively equal distribution of its pore volume across the range of pore diameters.

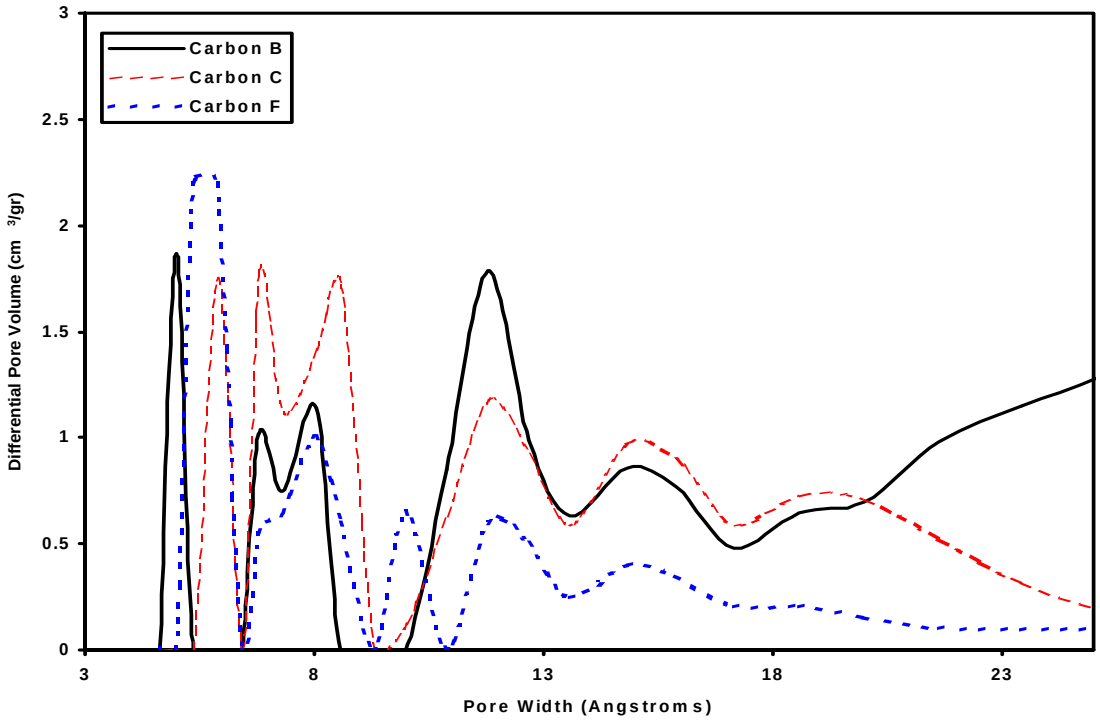

Figure 3: Pore size distribution of activated carbon materials as determined by Density Functional Theory.

3.2. Toluene Adsorption:

The toluene adsorption isotherms on the three activated carbons are compared in Figure 4. The highest surface area carbon, Carbon B, has the highest capacity for toluene at toluene concentrations greater than 3,000 ppmv. At lower toluene concentrations, the more microporous carbons have a higher adsorption capacity revealing the importance of micropores for removing VOCs at low concentrations. To further emphasize this point, we point out that at the lowest concentration evaluated, 5 ppmv toluene, Carbon F has the highest capacity for toluene. This carbon has the lowest total surface area of the three activated carbons evaluated here, but it has the highest micropore to total surface area ratio.

The apparent crossover in adsorption capacity with surface area and micropore area has been discussed previously.[12, 17, 25] It has also been shown before, that this crossover occurs at different contaminant concentrations for different contaminants. As can be seen in Figure 4, this crossover, also occurs at different concentrations of a contaminant when several different types of activated carbons are compared. For example, there are three crossover points in Figure 4. These crossovers occur at: 1) 3,000 ppmv of toluene for Carbon B and Carbon C; 2) 500 ppmv of toluene for Carbon B and Carbon F; and 3) 10 ppmv for Carbon C and Carbon F. These observations reveal that both the pore structure and surface chemistry play a pivotal role in determining adsorption capacity at low contaminant concentrations.

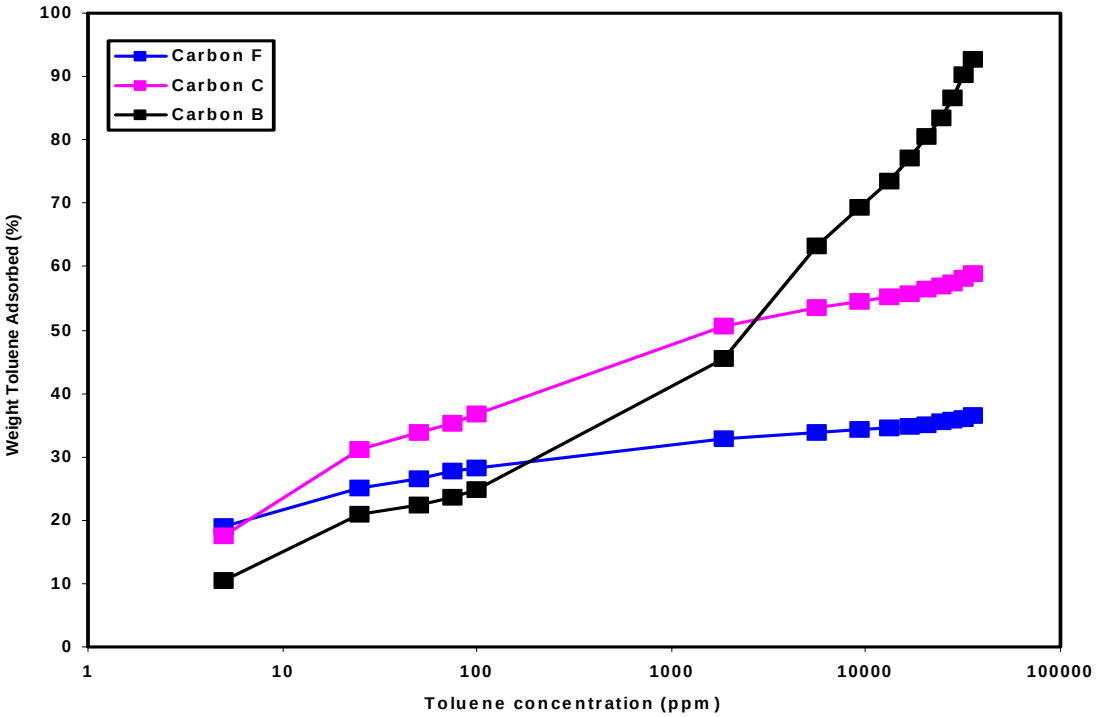

Figure 4: Toluene adsorption isotherms on three activated carbons.

3.3. Water Adsorption:

The water adsorption and desorption isotherms on the three activated carbons are given in Figure 5. Even at the high relative concentrations of water, 15-95 %RH, crossover in the adsorption and desorption capacities are clearly observed. At relative humidity's of less than 45 %, Carbon F, the lowest surface area carbon, is capable of adsorbing considerably more water than the other two activated carbons. However, at relative humidity's greater than 85 %, Carbon B, the highest total surface area carbon, has the greatest capacity. Although these results can be interpreted based solely on surface area, it will be shown below that the low relative humidity capacity is also dictated by the activated carbon surface basicity.

3.4. pH of the Carbon Surface:

Table 3 gives the activated carbon pH results. Carbon C has the most acidic surface and Carbon F has the most basic surface. Carbon B's surface is essentially neutral; however, this does not necessarily mean that this carbon's surface does not contain acidic and basic groups. These results suggest that the elevated water adsorption capacity of Carbon F at low relative humidity is due to basic nature of the carbon surface. Water is known to be a good hydrogen bond donor acid;[26] therefore, the basic sites on the carbon surface must be good hydrogen bond acceptors. In the case of water, these basic sites must still exert their influence on the carbon's adsorption capacity even at relative humidity's as high as 45 %.

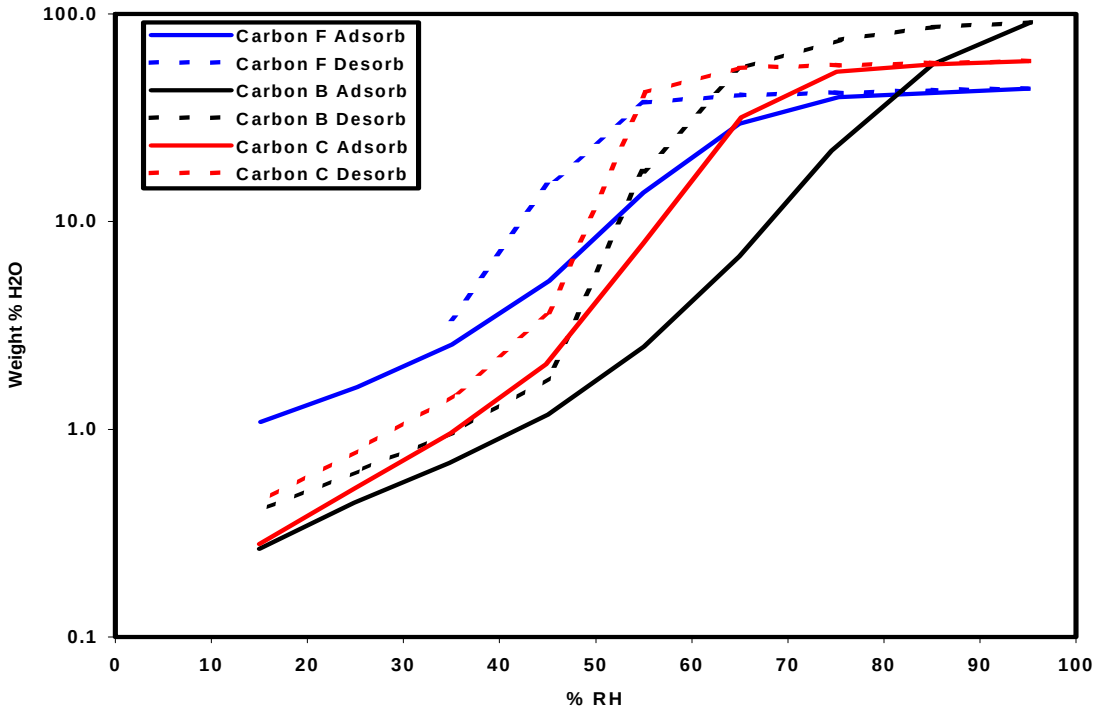

Figure 5: Water adsorption and desorption isotherms on three activated carbons.

Table 3: Activated Carbon pH and EDS results:

Activated Carbon	pH	EDS Results (Weight %)			
		Carbon	Oxygen	Sulfur	Silicon
Carbon B	6.44	93.0	7.0	ND[a]	ND[a]
Carbon C	4.63	91.0	8.4	0.5	0.1
Carbon F	8.89	88.4	10.4	ND[a]	ND[a]

a. Not detected.

3.5. *Energy Dispersive Spectroscopy of Carbon surface:*

The EDS results for the activated carbon materials are also given in Table 3. The most basic carbon, Carbon F, contains the highest level of oxygen. Therefore, these basic sites must primarily result from oxygen containing groups such as chromenes, pyrones, quinones, and ethers.[3] Carbon C, the most acidic carbon, contains an intermediate level of oxygen relative to the other two carbons. The oxygen present on the surface of Carbon C must give rise to acidic sites such as carboxylic acids, phenols, and hydroxyls. We note that Carbon C was the only carbon studied that contained other elements that were significant in the EDS analysis.

3.6. Inverse Gas Chromatography/Linear free energy relationships:

An easy method of comparing the adsorption on one activated carbon with another is to simply plot the elution temperature of the adsorbates on one activated carbon against their elution temperature on the other. Figures 6A, B, and C, make these comparisons for the three activated carbons studied here. These comparisons readily show that the energy of adsorption for all adsorbates on Carbon F is significantly higher than on the other two carbons.

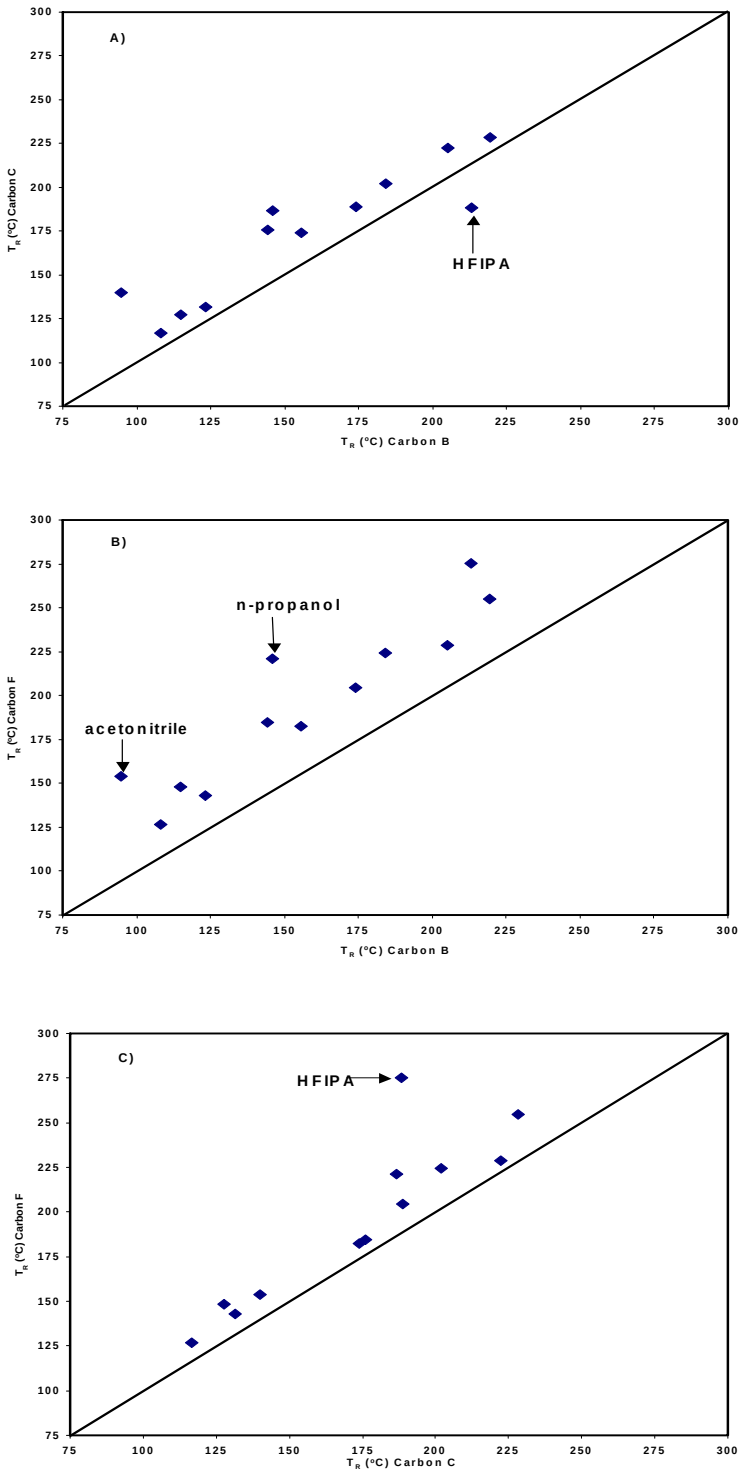

Figure 6: Comparison between the elution temperature of all adsorbates on each activated carbon. Diagonal line is the line of perfect agreement between the elution temperature on each of the two carbons being compared.

A useful way of viewing the elution temperature results is to plot them as a function of boiling point. When dispersive interactions dominate retention in chromatography, a linear relationship between retention and boiling

point, or carbon number, is generally obtained. However, when specific interactions are involved in the retention process, they tend to shift the polar adsorbates away from the linear relationship formed by the n-alkanes. Specific interactions between the adsorbates and the carbon surfaces we have studied are indicated in the following figure. Since there aren't any clear relationships with boiling point, it is clear that specific interactions play a significant role in the adsorption and desorption of adsorbates from these three activated carbons.

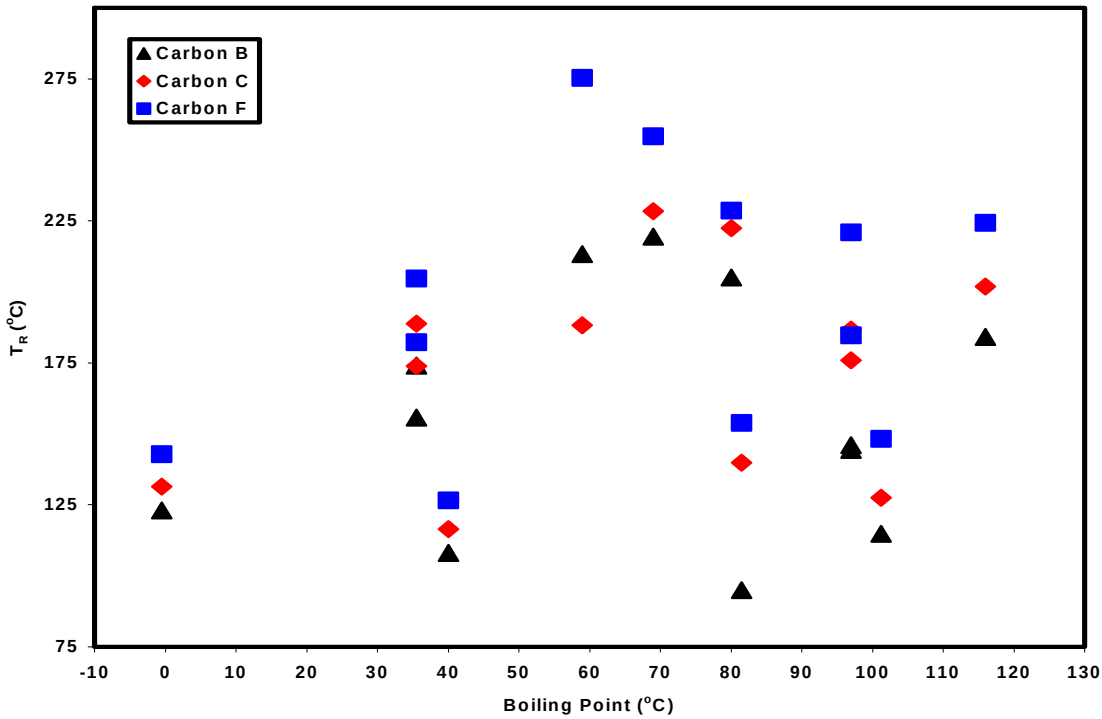

Figure 7: Elution temperature from activated carbons as a function of adsorbate boiling point.

Shown anther way, the significance of the specific interactions can be demonstrated using an approach similar to that given in Figure 1. The following figure compares the elution temperature from Carbon B as a function of the McGowan characteristic molecular volume, V_x. The n-alkanes are linear with adsorbate volume, thereby forming the reference line for the nonspecific free energy of adsorption. Since T_R for all of the adsorbates, other than the n-alkanes, fall above the alkane reference line, there must be specific interactions between the polar adsorbates and the surface of the activated carbons.

In our adsorbate training set, there are two homologous series, the n-alkanes and the nitriles. In Figure 7, the best fit regression line for these homolog series is also provided. As expected, there is essentially a perfect linear relationship with elution temperature and adsorbate size, or carbon number. Or in other words, the incremental change in T_R for a one carbon atom change in either the n-alkane or nitrile series results in a uniform step in temperature, or the free energy of adsorption. Since the slope of the two best fit lines are slightly different, the incremental step in the free energy of adsorption is different and is dictated by the presence of a functional group, for example in this specific case a nitrile group. Furthermore, the difference between the two regression lines decreases with increasing adsorbate volume, or carbon number, and these series will eventually merge at a specific adsorbate size. This indicates that as the carbon chain length for the nitrile series increases, its free energy of adsorption tends to that of the n-alkane reference line.

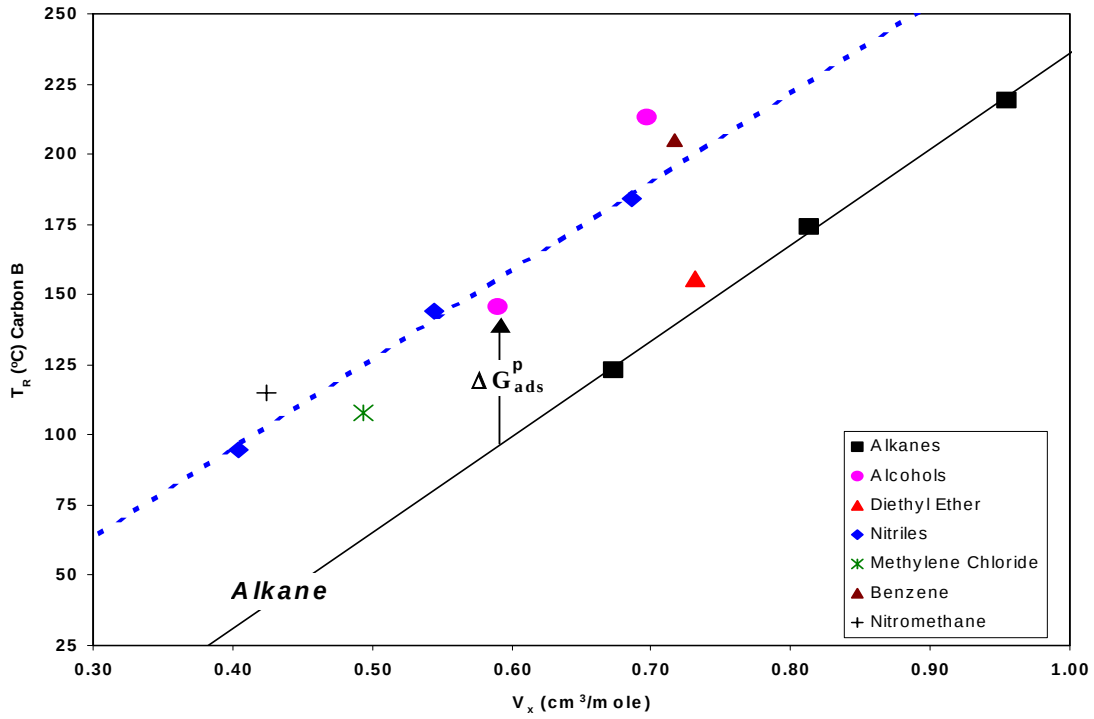

Figure 8: Elution temperature on Carbon B as function of adsorbate size.

The measured elution temperatures for the twelve probe adsorbates were regressed against the adsorbate descriptors using Equations 2 and 3. The results obtained using Equation 2 indicated that the surface dipolarity/polarizability and surface acidity, as indicated by significant **s** and **b** coefficients, were insignificant in the adsorption and desorption of adsorbates on all three activated carbons. It also suggested that the **r** coefficient, which indicates the ability of the carbon's surface to interact with adsorbate π- and n-electron pairs, is negative. Or in other words, these interactions were repulsive and decreased the retention of adsorbates on carbon surfaces, which doesn't make chemical sense.[8] Conversely, Equation 3, which uses V_x to represent the size of the adsorbate and its dispersive interactions with the carbon surface, gave the best fits to the elution temperature results and coefficients that make good chemical sense given the expected adsorbate-carbon surface interactions.

The LFER regression equation coefficients obtained using equation 3 are given in Table 4.

Table 4: LFER regression coefficients for elution temperatures from the three activated carbons using equation 3:

Activated Carbon	SP	m	r	s	b	a	R[a]	s.d.[b]	n[c]
Carbon B	-126.2	365.1	44.0	66.0	0	71.8	0.991	7.2	12
Carbon C	-85.7	325.8	58.6	50.8	47.4	39.6	0.957	14.6	12
Carbon F	-97.1	363.7	33.5	80.5	0	116.1	0.965	15.5	12

a. correlation coefficient.
b. standard deviation of the regression.
c. number of adsorbates in regression.

The LFER regression coefficients using Equation 3 indicate that dipolarity/polarizability and hydrogen bonding interactions are significant adsorbate-activated carbon interactions on all three activated carbons evaluated here. We also note that the **r** coefficient is positive indicating favorable interactions between the carbon surface and the adsorbate's π- and n-electron pairs. These results are contrary to those previously presented using Equation 2. Equation 2 was also evaluated here, but gave significantly poorer fits, an unfavorable/negative **r** coefficient was obtained, dipolarity/polarizability interactions were insignificant, and all three activated carbon surfaces were deemed to by slightly basic as revealed through a positive **a** coefficient. Obviously, the use of Equation 2 for interpreting the adsorbate-activated carbon surface interactions for the three activated carbons we have studied is not recommended.

We recommend the use of Equation 3, which uses V_x to represent the adsorbate size, which also scales the adsorbates dispersive interactions. In support of this we point out that diffusion of an adsorbate into an activated carbon micropore and interaction with the surface functional groups does not involve any cavity formation process in either the gas or the solid phase as is modeled by the use of L^{16} in Equation 2. Furthermore, the adsorption of adsorbates at low concentrations only requires that it be able to reach the high-energy sites on the activated carbon surface. The capability of an adsorbate to do this is dictated by its size and shape relative to the size and shape of the pores that contain these sites.

The LFER results given in Table 4 indicate that although the primary contribution to the adsorption and desorption free energy is the adsorbate's size, specific interactions also play a significant role. Due to the similarity of the **m** coefficients of the three activated carbons, only minor adsorption and desorption selectivity differences for adsorbates between these activated carbons can be attributed to nonspecific interactions. The major differences between the free energy of adsorption and desorption of adsorbates on these activated carbons lie in their ability to enter into specific interactions with the adsorbates.

Specific interactions between the adsorbates and the activated carbon surface are demonstrated by the magnitude of the **r**, **s**, **b**, and **a** coefficients. The ability of these carbon surfaces to interact with adsorbate π- and n-electron pairs, **r** coefficient, and an adsorbates dipolarity/polarizability, **s** coefficient, is very similar and result in only minor differences in the free energy of adsorption and desorption. Therefore the major selectivity differences between the activated carbons must lie in their ability to donate and accept hydrogen bonds, **b** and **a** coefficients, respectively. Carbon C is the only activated carbon that has a significant number of strong hydrogen bond donor sites as revealed by the **b** coefficient being insignificant on Carbon's B and F. The ability of these carbon surfaces to accept hydrogen bonds from adsorbates, **a** coefficient, spans a large range indicating large differences exist in the hydrogen bond basicity of the surfaces.

In Figure 9, we show that the **s** and **b** coefficients correlate very well with the carbon surface pH. This suggests that similar groups are responsible for the carbon surface dipolariy/polarizability, hydrogen bond donating ability, and pH. Further analysis is required to draw any further conclusions.

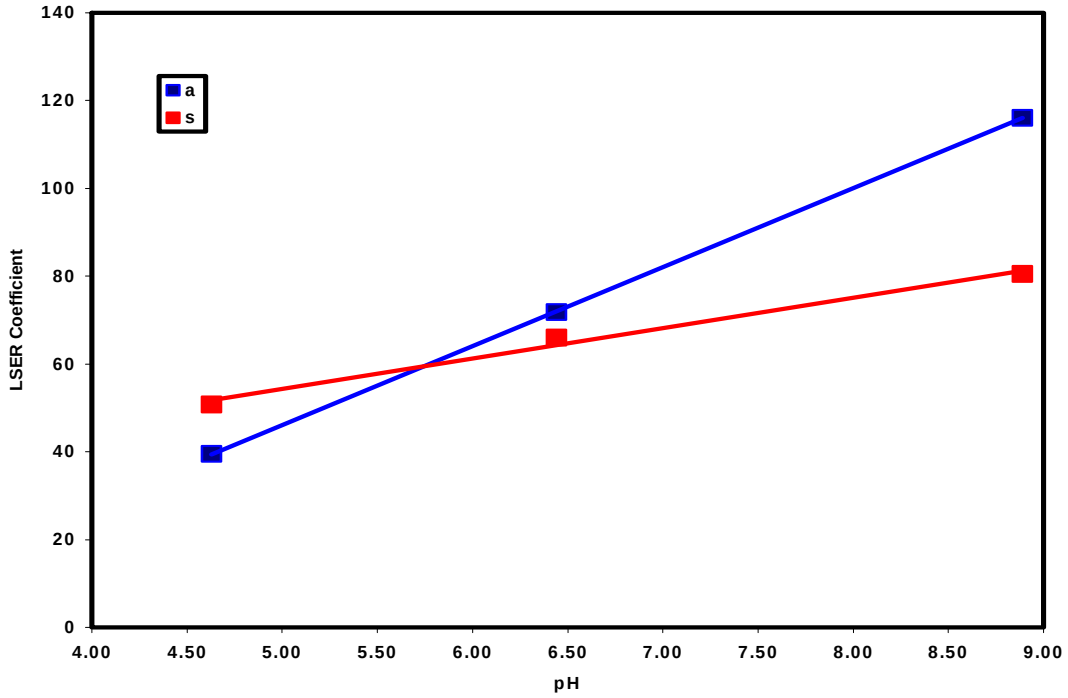

Figure 9: Magnitude of the LFER coefficient as a function of the activated carbon surface pH.

3.7. Breakthrough Curves and LFER Predictions:

The standard deviation of the LFER equations given in Table 4, reveals that the elution temperature for adsorbates present at infinitely dilute concentrations can be estimated on all three activated carbons to better than 15°C. Therefore differences between the free energy of adsorption and desorption, hence the selectivity, of adsorbates on the three activated carbons can possibly be predicted using the LFER equations. In an attempt to demonstrate the benefits of screening activated carbon selection for a specific low concentration filtration application, we have measured the breakthrough curves for a series of seven Test VOCs found in typical chemical filter applications. The LFER equations were used to predict the expected selectivity of the three activated carbons for these VOCs and the predictions are compared with the actual breakthrough performance test results. In the cases presented herein we use selectivity as being synonymous with capacity.

In Table 5 we provide the elution temperature estimates for the seven Test VOCs and the predicted selectivity/capacity order of the specific VOC on the three activated carbons.

Table 5: Estimated elution temperature of Test VOCs.

Test VOC	Estimated Elution Temperature (°C)			Predicted Selectivity
	Carbon B	Carbon C	Carbon F	
Sulfur Dioxide	80	98	127	B<C<F
Ammonia	-11	43	28	B<F<C
n-Propane	68	87	96	B<C<F
Toluene	248	262	277	B<C<F
Ethanol	103	134	151	B<C<F
Acetaldehyde	75	114	112	B<F≈C
Water	23	41	95	B<C<<F

In Figures 10-15 we provide comparisons of the breakthrough curves for each of the seven Test VOCs on the three activated carbons, except for water. The water results are extrapolated from the adsorption isotherms presented in Figure 5.

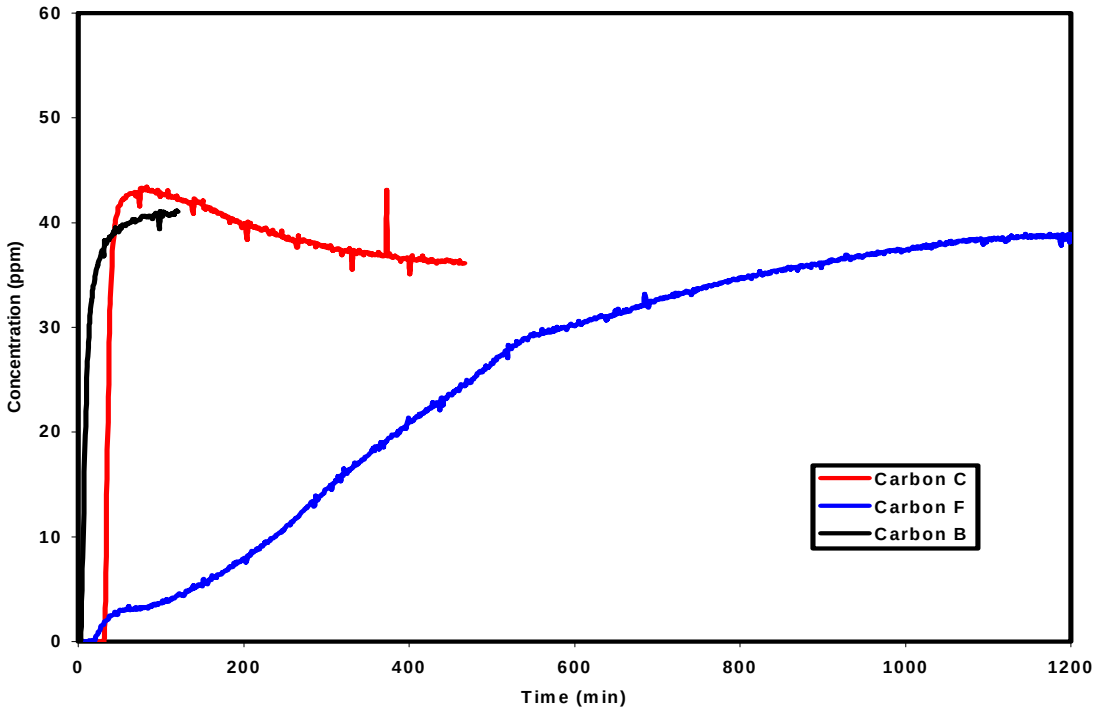

Figure 10: Breakthrough curves for 50 ppmv sulfur dioxide on the three activated carbons.

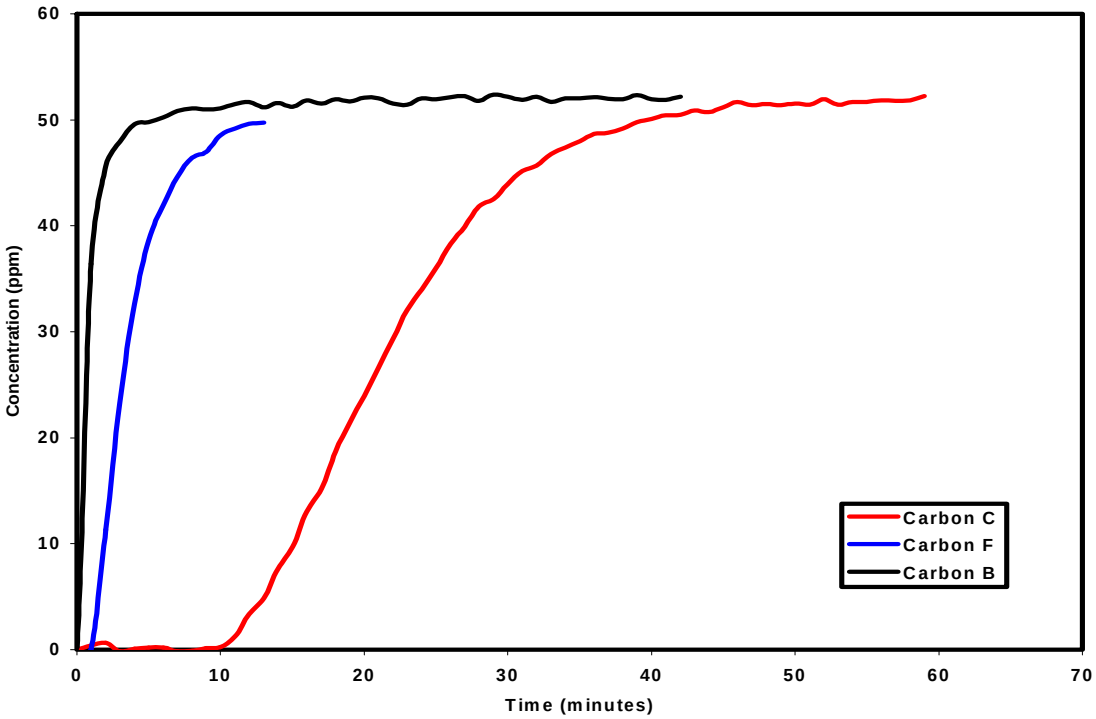

Figure 11: Breakthrough curves for 50 ppmv ammonia on the three activated carbons.

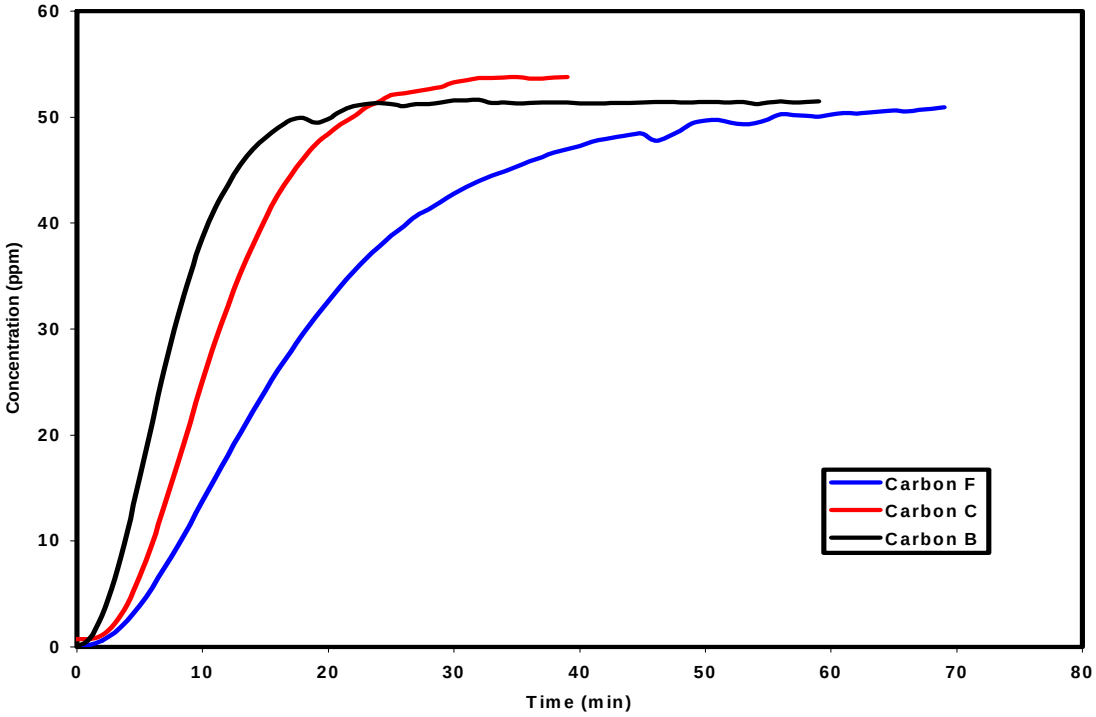

Figure 12: Breakthrough curves for 50 ppmv n-propane on the three activated carbons.

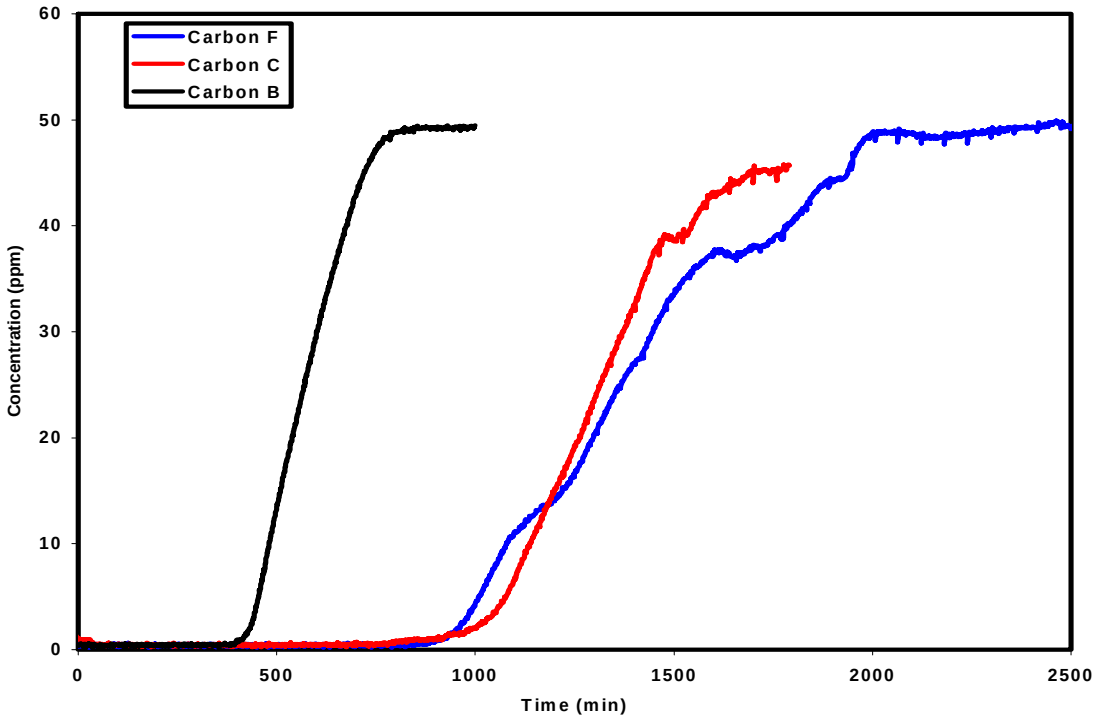

Figure 13: Breakthrough curves for 50 ppmv toluene on the three activated carbons.

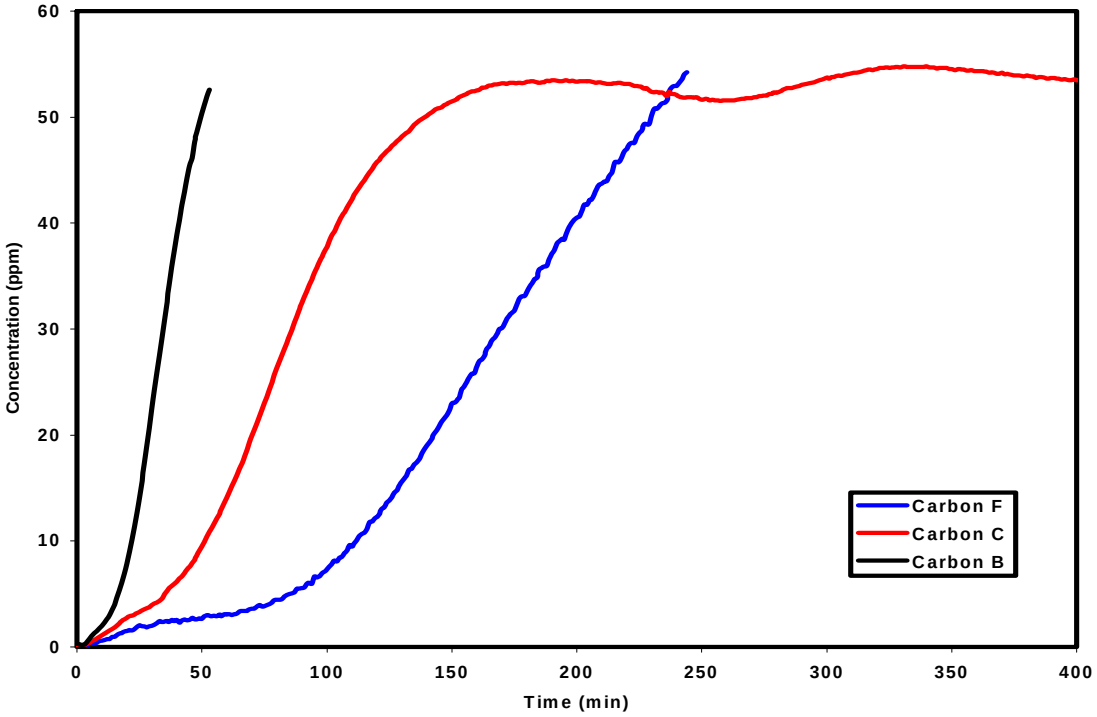

Figure 14: Breakthrough curves for 50 ppmv ethanol on the three activated carbons.

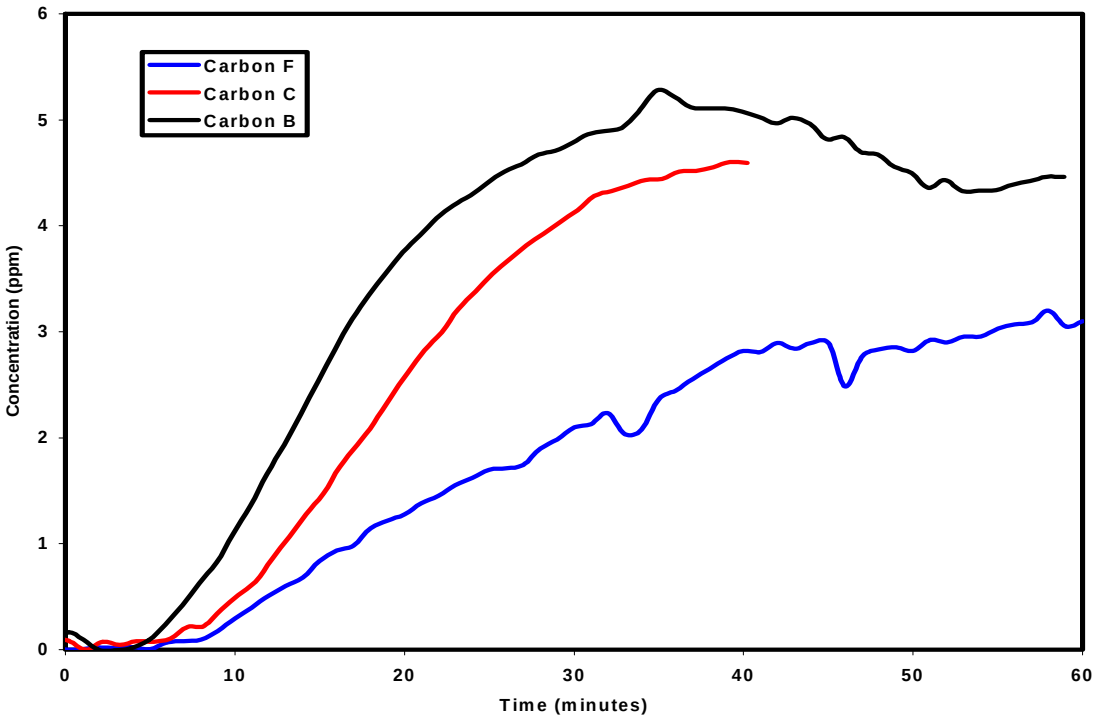

Figure 15: Breakthrough curves for 6 ppmv acetaldehyde on the three activated carbons.

The order of the selectivity/capacity for the seven Test VOCs on the three activated carbons was predicted perfectly using the LFER equations. So, by only considering the magnitude of the adsorbate-activated carbon interactions that govern the adsorption and desorption process at low adsorbate concentrations, we were able to screen activated carbon materials and make the best choice for the specific adsorbate. More importantly, these effective predictions were made without including any consideration for the activated carbon surface area or pore size; however, these effects are convoluted into the LFER equation coefficients and intercept. We note that the lowest surface area activated carbon, Carbon F, was the best performing activated carbon, from a capacity perspective, for all but one of the seven Test VOCs.

Since LFER descriptor databases typically contain descriptors for on the order of 3,000 contaminants, this screening approach can be quite a powerful tool for selecting appropriate adsorbents. Furthermore, since low VOC concentration breakthrough tests take considerable amounts of time and manpower, the use of these LFER equations can provide a significant time and cost savings

4. SUMMARY

In conjunction with a simple temperature programmed IGC method using multiple probe adsorbates, it has been demonstrated that the LFER approach is a rapid method for screening adsorbents for chemical filter design. LFER equations were developed from the measured elution temperature of twelve probe adsorbates. These equations have been used to effectively rationalize the adsorbate-activated carbon surface interactions at low adsorbate concentrations. The LFER regression coefficients were shown to have chemical significance by comparing them with other measurements of the activated carbon surface properties. By using the LFER equations to predict the performance of three activated carbons for the removal of seven Test volatile organic contaminants, it has been shown that understanding the adsorbate-activated carbon surface interactions is imperative when making chemical filter choices for applications involving low adsorbate concentrations.

5. REFERENCES

1. F. Rouquerol, J. Rouquerol, and K. Sing, *Adsorption by Powders and Porous Solids*, Academic Press, 1999.
2. K. E Noll, V. Gounaris, and W. S. Hou, *Adsorption Technology for Air and Water Pollution Control*, Lewis Publishers, 1992.
3. R. C. Bansal, J-B. Donnet, F. Stoeckli, *Active Carbon*, Marcel Dekker, Inc., 1988.
4. R. T. Yang, *Gas Separation by Adsorption Processes*, Butterworths Publishers, 1987.
5. P. Burg, P. Fydrych, J. Bimer, P. D. Salbut, and A. Jankowska, "Comparison of three active carbons using LSER modeling: prediction of their selectivity towards pairs of volatile organic compounds (VOCs)" *Carbon*, 40, 2002, 73-80.
6. H. Balard, E. Brendle, and E. Papirer, "Determination of the acid-base properties of solid surfaces using Inverse Gas Chromatography: Advantages and Limitations" in *Acid-Base Interactions: Relevance to Adhesion Science and Technology, Volume 2*, K. Mittal editor, 2000.
7. T. Bandosz, "Effect of pore structure and surface chemistry of virgin activated carbons on removal of hydrogen sulfide," *Carbon*, 37, 1999, 483-491.
8. J. H. Park, Y. K. Lee, J-B. Donnet, "A Study of Solid Surface Polarity Using Inverse Gas Chromatographic Retention Data," *Chromatographia*, 33, 1992, 154-158.
9. C. Vagner, G. Finqueneisel, T. Zimny, P. Burg, B. Grzyb, J. Machnikowski, and J. V. Weber, "Characterization of the surface properties of nitrogen-enriched carbons by inverse gas chromatography methods," *Carbon*, 41, 2003, 2847-2853.
10. J. Jagiello, T. J. Bandosz, and J. A. Schwarz, "Application of inverse gas chromatography at infinite dilution to study the effects of oxidation of activated carbons," *Carbon*, 30, 1992, 63-69.
11. P. Burg, M. H. Abraham, and D. Cagniant, "Methods of determining polar and non-polar sites on carbonaceous adsorbents. The contribution of the linear solvation energy relationship approach," *Carbon*, 41, 2003, 867-879.
12. A. J. Dallas, L. Ding, J. D., Joriman, "Using Adsorption Isotherms to Find the Best Activated Carbon to Remove Volatile Organic Contaminants," *Donaldson internal publication*, 2003.
13. C. L. Mangun, K. R. Benak, M. A. Daley, and J. Economy, "Oxidation of Activated Carbon Fibers: Effect of Pore Size, Surface Chemistry, and Adsorption Properties," *Chemistry of Materials*, 11, 1999, 3476-3483.
14. I. I. Salame and T. Bandosz, "Interaction of water, methanol, and diethyl ether molecules with the surface of oxidized activated carbon," *Molecular Physics*, 100, 2002, 2041-2048.
15. H. Tamon and M. Okazaki, "Influence of Acidic Surface Oxides of Activated Carbon on Gas Adsorption Characteristics," *Carbon*, 34, 1996, 741-746.
16. D. W. VanOsdell, M. K. Owen, and L. B. Jaffe, "VOC Removal at Low Contaminant Concentrations using Granular Activated Carbon," *J. Air & Waste Management Association*, 46, 1996, 883-890.
17. K. L. Foster, R. G. Fuerman, J. Economy, S. M. Larson, and M. J. Rood, "Adsorption Characteristics of Trace Volatile Organic Compounds in Gas Streams onto Activated Carbon Fibers," *Chemistry of Materials*, 1992, 4, 1068-1073.
18. C. L. Mangun, M. A. Daley, R. D. Braatz, and J. Economy, "Effect of Pore Size on Adsorption of Hydrocarbons in Phenolic-Based Activated Carbon Fibers," *Carbon*, 36, 1998, 123-132.
19. T. J. Bandosz, J. Jagiello, and J. A. Schwarz, "Effect of Surface Chemistry on Sorption of Water and Methanol on Activated Carbons," *Langmuir*, 12, 1996, 6480-6486.
20. G. Guicohon and C. L. Guillemin, *Quantitative Gas Chromatography*, Elsevier Science Publishing, 1988.
21. M. N. Belgacem and A. Gandini, "Inverse Gas Chromatography as a Tool to Characterize Dispersive and Acid-Base Properties of Fibers and Powders," in *Interfacial Phenomena in Chromatography; Surfactant Science Series Vol. 80*, edited by Emile Pefferkorn, Marcel Dekker, 1999.
22. M. H. Abraham, G. J. Buist, P. L. Grellier, R. A. McGill, R. M. Doherty, M. J. Kamlet, R. W. Taft, and S. G. Maroldo, "Solubility Properties in Polymers and Biological Media. A New Method for the Characterisation of the Adsorption of Gases and Vapours on Solids," *J. of Chromatography*, 409, 1987, 15-27.
23. M. H. Abraham and D. P. Walsh, "Hydrogen Bonding XXIII. Application of the new solvation equation to log V_g values for solutes on carbonaceous adsorbents," *J. Chromatography*, 627, 1992, 294-299.

24. A. W. McMahon, D. G. Kelly, and P. J. McLaughlin, “Characteristics of hererogeneous solid surfaces by multiple probe, temperature-programmed inverse gas chromatography (IGC). A feasibility study,” *Analyst*, 127, 2002, 17-21.
25. K. L. Graf, M. J. Rood, S. M. Larson, and J. Economy, *Proceedings of Air & Waste Management 86th Annual Meeting*, June 1993, 93-MP-3.05, pgs. 2-11.
26. M. H. Abraham, J. Andonian-Haftvan,, G. S. Whiting, and A. Leo, “Hydrogen Bonding. Part 34. The Factors that Influence the Solubility of Gases and Vapours in Water at 298K, and a New Method for its Determination,” *J. Chem. Soc. Perkin Trans. 2*, 1994, 1777-1791.
27. M. H. Abraham, “Scales of Hydrogen-Bonding: Their Construction and Application to Physicochemical and Biological Processes,” *Chemical Society Reviews*, 1999, 73-83.
28. M. H. Abraham and J. C. McGowan, “The Use of Characteristic Volumes to Measure Cavity Terms I Reversed Phase Liquid Chromatography,” *Chromatographia*, 23, 1987, 243-246.
29. J. P. Oliver, W. B. Conklin, and M. v. Szombathely, “Determination of Pore Size Distribution from Density Functional Theory: A Comparison of Nitrogen and Argon Results,” *in Characterization of Porous Solids III, Studies in Surface Science and Catalysis*, editors J. Rouquerol, F. Rodriquez-Reinoso, K. S. W. Sing, and K. K. Unger, 87, 1994, 81-89.
30. P. A. Webb and C. Orr, *Analytical Methods in Fine Particle Technology*, Micromeritics, 1997.